Thermal-Optical Design of a Geodetic Satellite for One Millimeter Accuracy

David A. Arnold
Smithsonian Astrophysical Observatory, Cambridge, MA, U.S.A. (retired)

Abstract:

The LAGEOS satellites use a 1.5 inch uncoated retroreflector (cube corner). The design studies done for LAGEOS in the early 1970s showed that using smaller cubes would result in greater accuracy and lower thermal gradients. The design goal for LAGEOS was 5 millimeters. Despite the problems the simulations showed that the accuracy goal could be met using 1.5 inch cubes. Using smaller cubes would require having a much larger number of cubes to obtain the necessary cross section. This would have a significant cost impact. Since the design goal could be met with 1.5 inch cubes LAGEOS used the 1.5 inch cubes for financial reasons.

The recent development of COTS (Commercial Off-The-Shelf) cube corners has eliminated cost as an obstacle to using smaller cubes. The COTS cubes have no dihedral angle offset. However, no offset is needed if the size is chosen properly. At Lageos altitude a 1.0 inch cube with no dihedral angle offset maximizes the cross section on the first diffraction ring of an uncoated cube.

Testing and analysis of a set of 10 COTS cubes done by Ludwig Grunwaldt and Reinhart Neubert shows good optical performance. The cubes are inexpensive and are manufactured in bulk. Simulations show that the systematic range errors on the order of a half millimeter are possible, at least in principle. Adjustments to accommodate the holding and ejection system can result in some loss of uniformity with incidence angle on the satellite.

Keywords: Lares-2; Lageos; retroreflectors; COTS cubes; laser ranging

David A. Arnold
david-arnold@earthlink.net, Phone: 617-924-6812, Website: www.davidarnoldresearch.org

Contents:

1. Basic principles.

The return from a retroreflector depends on the wavefront exiting the cube corner. For a perfect reflector, the exiting wavefront is flat with constant phase across the aperture. The far field pattern for a perfect circular retroreflector is the well known Airy pattern. The width of the Airy pattern is proportional to the wavelength divided by the diameter of the cube corner.

The far field pattern is shifted by velocity aberration given by 2v/c where v is the velocity of the satellite and c is the speed of light. In order to get a return, the pattern has to be wide enough to account for velocity aberration. The simplest way to obtain the necessary beam spread is to adjust the size to get the proper beam spread.

In a solid uncoated cube corner, there are three primary physical effects that alter the phase front.

1. Phase changes due to total internal reflection at the back faces.
2. Dihedral angle offsets.
3. Changes in index of refraction due to thermal gradients.

The phase changes due to total internal reflection results in 6 lobes around the central peak of the diffraction pattern. The size of the cube corner can be adjusted so that velocity aberration puts the receiver on this ring of 6 spots or on the central peak.

Dihedral angle offsets are not needed and create a complicated diffraction pattern. In particular, the sum of the phase changes due to total internal reflection and dihedral angle offsets creates an asymmetric diffraction pattern when linear polarization is used. There will always be some small dihedral angle offsets due to manufacturing errors.

The effect of thermal gradients can be minimized in two ways:

1. Keep the optical path length as short as possible by using small cube corners.

2. Keep the cube corner as cold as possible to reduce thermal radiation from the front face. The cube corner should be thermally decoupled from the core by using a floating mount to reduce

conduction, and a low emissivity of the mounting cavity to reduce radiative heating of the cube corner.

Keeping the cube corner cold requires adjusting the thermal parameters of the core and the cavity to minimize the temperature of the cube corner. Section 7 gives equations for doing this.

2. Centroid vs incidence angle

Simulations have been done for an array with rings of cubes separated by 12 degrees on a 20.1 cm radius sphere. The array geometry is given in the table below. There are 288 cubes.

Ring	Latitude	# of CCRs
1	90	1
2	78	6
3	66	12
4	54	18
5	42	22
6	30	26
7	18	29
8	6	30
9	-6	30
10	-18	29
11	-30	26
12	-42	22
13	-54	18
14	-66	12
15	-78	6
16	-90	1

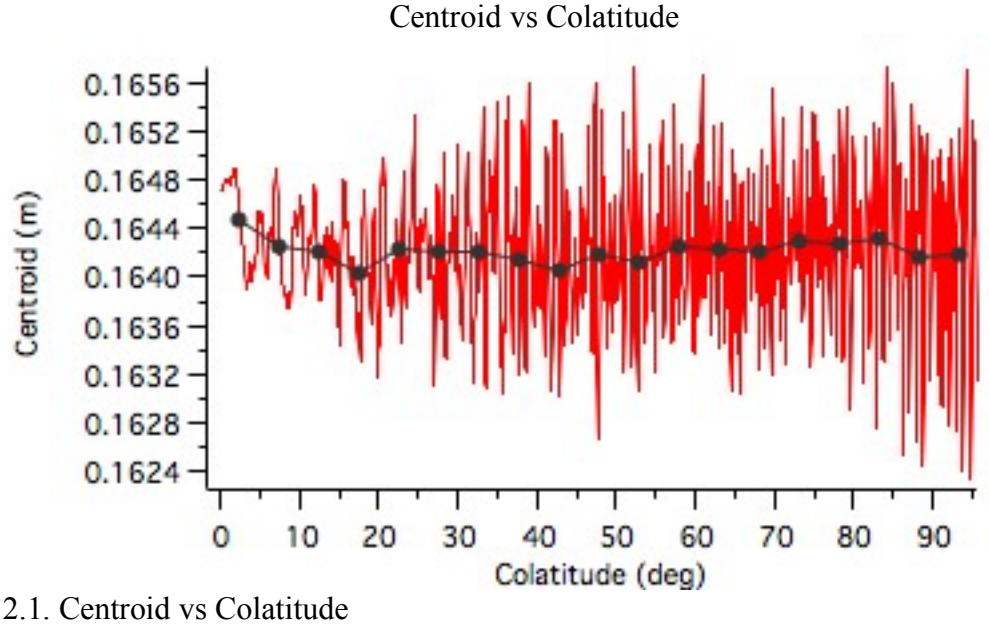

Figure 2.1. Centroid vs Colatitude

Statistics for the red line (all points)

Minimum	Maximum	Max - Min	Average	Rms
0.1623	0.1657	0.0034	0.1642	0.0006

Statistics for the black line (average over sets of 72 points)

Phi	minimum	Phi	maximum	max-min
17.6050	0.1640	2.4850	0.1645	0.0004

3. Thermal problems.

Thermal testing of 1.5 inch cube corners shows significant thermal distortion of the diffraction pattern. Thermal distortion causes unmodeled changes in the range correction. The plots are full scale 110 μrad.

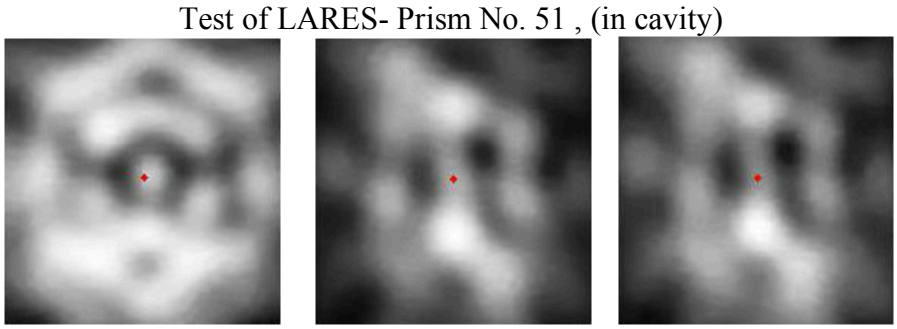

Figure 3.1. Diffraction patterns with thermal gradients

4. Polarization asymmetry.

In an uncoated cube, there is an interaction between dihedral angle offsets and phase changes due to total internal reflection. This results in an asymmetrical diffraction pattern if linear polarization is used. The pattern has circular symmetry for circular polarization. The asymmetry can be virtually eliminated if no dihedral angle offset is used. The offset of 1.25 arcsec in the 1.5 inch cubes is necessary to account for velocity aberration. If 1.0 inch uncoated cubes are used the diffraction pattern is wide enough to account for velocity aberration without the need for a dihedral angle offset.

Simulations have been done comparing 1.5 and 1.0 inch uncoated cubes. The first design uses 204 1.5 inch cubes on a 200 mm radius satellite. The second design uses 303 1.0 inch cubes on a 202 mm radius satellite. The range correction and cross section matrices are irregular at a single incidence angle on the satellite for both circular and linear polarization. The matrices have been averaged over 2520 orientations of the satellite. When this is done a circular pattern shows up for circular polarization and an asymmetric pattern for linear polarization The magnitude of the range correction is different for the two designs because the optical path length is different in

the different size cubes and the radius of the satellite is slightly different. The scale of the figures below is -50 to +50 μrad.

Centroid matrices

1.5 inch cubes

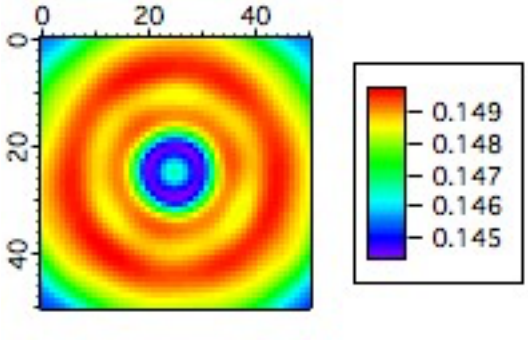

Circular polarization
Figure 4.1

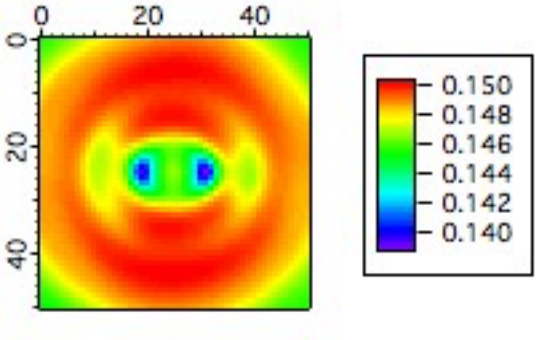

Linear polarization
Figure 4.2

1.0 inch cubes

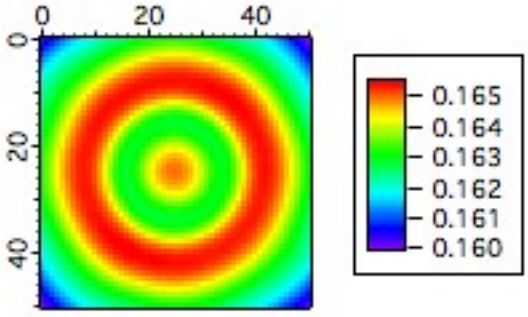

Circular polarization
Figure 4.3

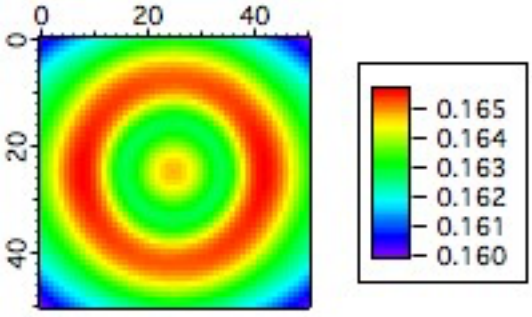

Linear polarization
Figure 4.4

Circular polarization produces a circular pattern for both size cubes. The pattern is not completely circular for the 1.5 inch cubes even with averaging over many incidence angles. The pattern for 1.0 inch cubes has good circular symmetry.

Linear polarization produces an asymmetric pattern for the 1.5 inch cubes with a dihedral angle offset of 1.25 arcsec. For the 1.0 inch cubes with no dihedral angle offset the pattern is nearly circular with linear polarization. There is a very small remaining asymmetry that is less than the accuracy goal for the satellite. The scale is -50 to +50 μrad.

Cross section matrices

1.5 inch cube

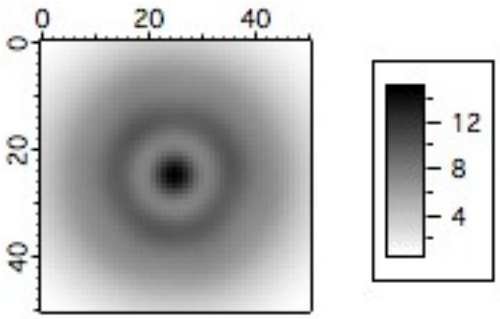

Circular polarization
Figure 4.5

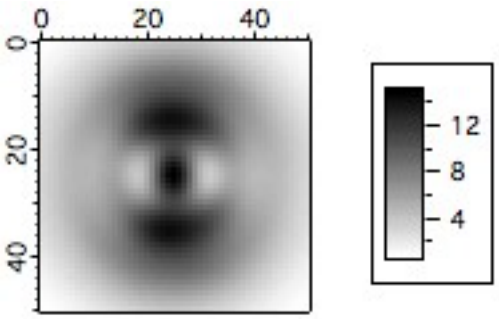

Linear polarization
Figure 4.6

1.0 inch cube

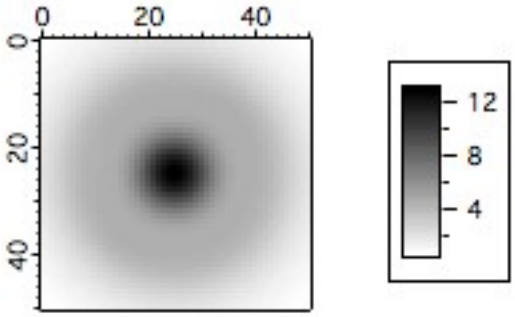

Circular polarization
Figure 4.7

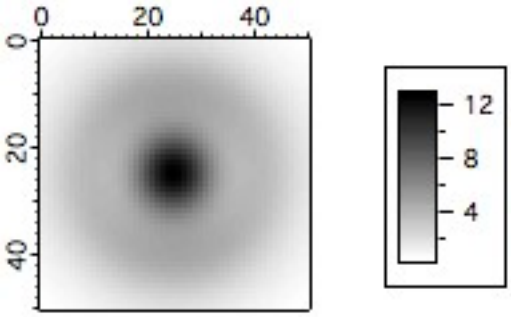

Linear polarization
Figure 4.8

The pattern with linear polarization is asymmetric for the 1.5 inch cubes but symmetric for the 1.0 inch cubes.

The maximum and minimum values of the centroid have been computed around circles of increasing radius in the far field. The asymmetry has been computed as the maximum minus the minimum. This difference has been plotted vs the magnitude of the velocity aberration.

Comparison of the asymmetry in the centroid

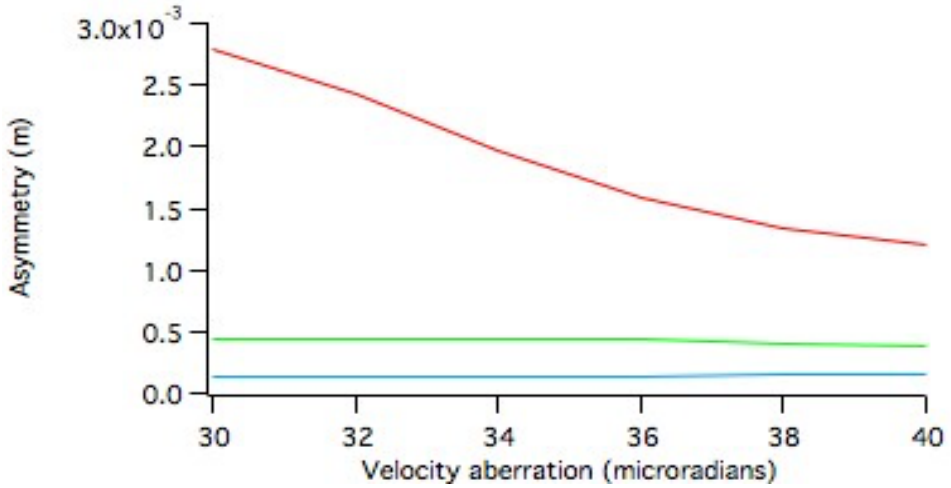

Figure 4.9. Asymmetry vs velocity aberration

Red (top) = 1.5 inch linear, Green (middle) = 1.0 inch linear, Blue (bottom)= 1.0 inch circular
With the 1.0 inch cubes the asymmetry is less than .5 mm.

5. Centroid vs velocity aberration.

The proposed design minimizes the variation of the centroid with velocity aberration by choosing the size of the cube to place the velocity aberration on a peak in the pattern. The results are plotted in the figures below. The velocity aberration varies between about 32 and 40 microradians. Linear vertical polarization is used.

Centroid vs velocity aberration

1.5 inch cube

Red (middle) = average, Green (bottom) = minimum, Blue (top) = maximum

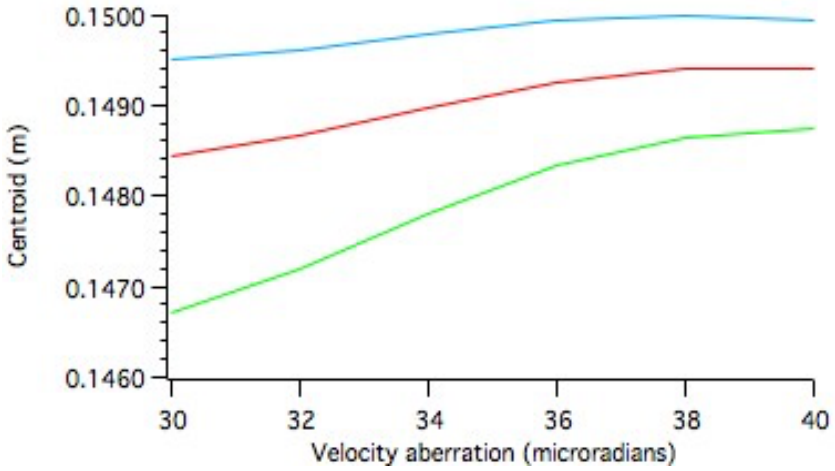

Figure 5.1. Centroid vs velocity aberration

1.0 inch

Red (middle) = average, Green (bottom) = minimum, Blue (top) = maximum

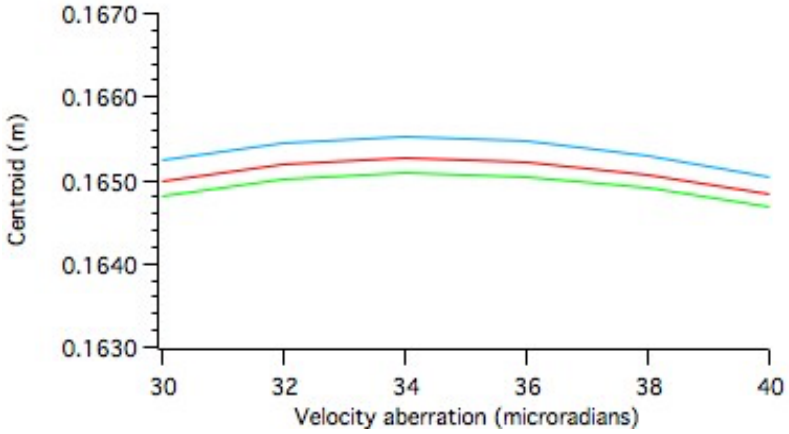

Figure 5.2. Centroid vs velocity aberration

The average (red curve) for the 1.5 inch cube changes by .74 mm from 32 to 40 microradians. However, the asymmetry of the pattern causes significant range errors. The change of the red curve is .47 mm for the 1.0 inch cube with very little asymmetry. This is within the accuracy goal of one millimeter. A correction could be applied as a function of velocity aberration.

6. Thermal simulations

If there were no thermal gradients the range correction would be constant. It could be measured in the lab before launch. It could be computed theoretically using the parameters of the cube corners and the measured dihedral angle offsets. The average cross section vs velocity aberration is the same for either a positive or negative dihedral angle offset if there are no thermal gradients. As a measure of the effect of thermal gradients the cross section vs velocity aberration has been computed for a positive and a negative dihedral angle offset under various thermal conditions.

Antonio Paolozzi has provided four thermal simulations under different conditions for a 1.0 inch uncoated cube. The output of the thermal simulations is a three-dimensional matrix giving the temperature distribution in the cube. The first step is to do a ray tracing to get the phase front due to the thermal gradients. The next step is to add phase changes due to dihedral angle offsets and total internal reflection. The far field pattern is computed from the phase front. The pattern is processed to compute the average cross section vs velocity aberration. Three simulations have been run for each case. The reference case is with a dihedral angle offset of either + or - 1.25 arcsec with no thermal gradient. This is compared to the cross section vs velocity aberration with a + and - dihedral angle offset and thermal gradients. The phase front due to a thermal gradient may be either primarily concave or primarily convex. The phase front for a dihedral angle offset is either concave or convex depending on the sign of the dihedral angle offset. A dihedral angle offset can either add to the effect of a thermal gradient or partially cancel it.

In the figures below, the average cross section is plotted vs the magnitude of the velocity aberration for a single cube corner. The thermal simulation is done first with the Italian program and second with my own thermal simulation, Thermal2.

Floating mount
Case 11, Italy program
Cube temperature 259 K, core 303 K, cavity e=.07
Red (middle) = dihedral angle 1.25 arcseconds, isothermal
Green (upper) = -1.25 with thermal gradient, Blue (lower) = +1.25, with thermal gradient

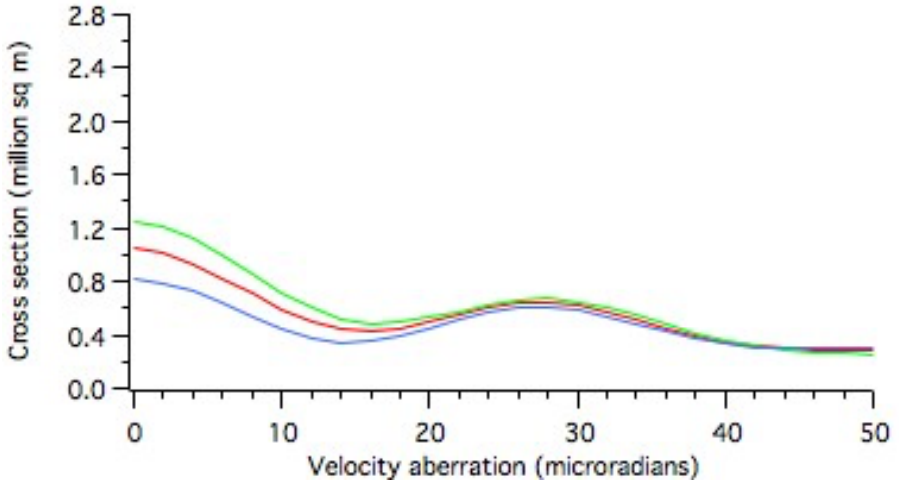

Figure 6.1a.

microrad	−1.25	+1.25	diff	fraction
32	0.60496278	0.54032960	.06463	.1068

Table 6.1a.

Case 11, Program Thermal2
Cube temperature 250 K

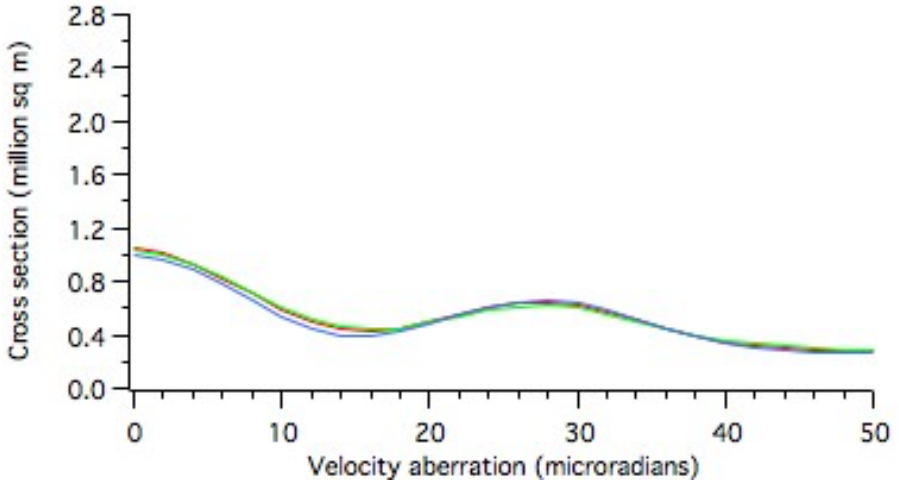

Figure 6.1b.

microrad	−1.25	+1.25	diff	fraction
32	0.55985671	0.58590446	.02604	.0444

Table 6.1b. Fraction is the ratio of diff to the largest cross section

Mount conduction .02 watts/deg K
Case 12, Italy Program
Cube temperature 293 K, core 303 K, emissivity e=.07
Red (middle) = dihedral angle 1.25 arcseconds, isothermal
Green (upper) = -1.25, Blue (lower) = +1.25, with thermal gradient

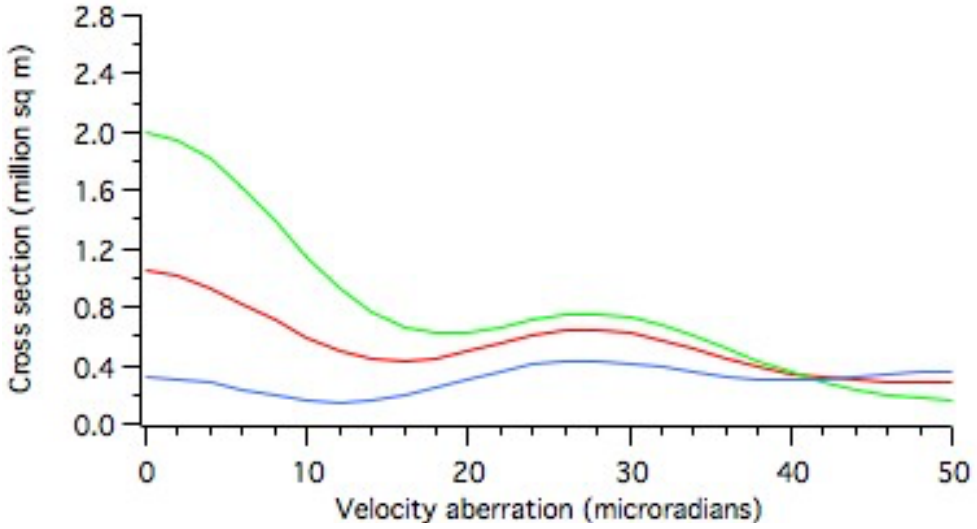

Figure 6.2a.

microrad	-1.25	+1.25	diff	fraction
32	0.68581183	0.38626526	.2995	.4368

Table 6.2a.

Case 12, Program Thermal2
Cube temperature 293 K

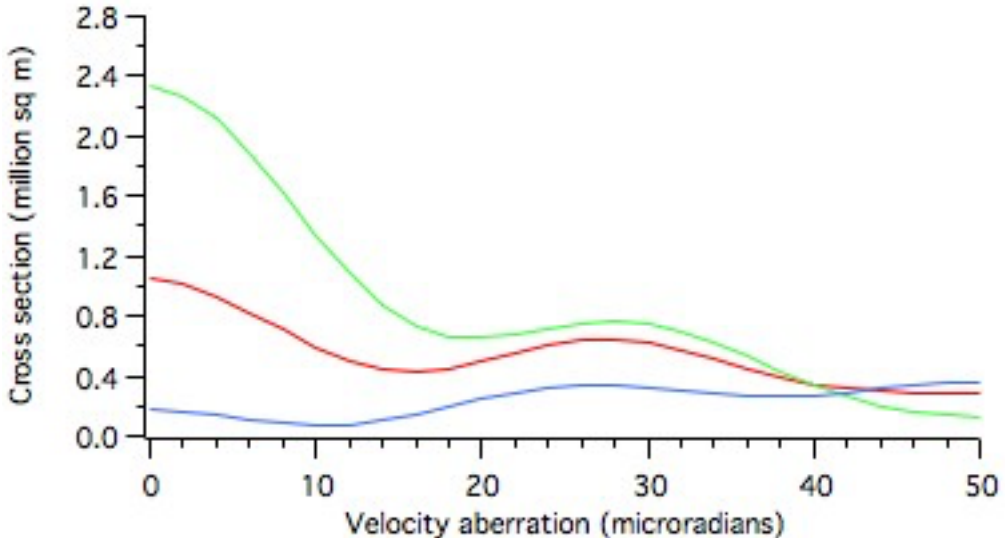

Figure 6.2b.

microrad	-1.25	+1.25	diff	fraction
32	0.69658931	0.30281921	.3937	.5653

Table 6.2b.

Floating mount
Case 16, Italy Program
Cube temperature 359 K, core 413 K, emissivity e=.29
Red (middle) = dihedral angle 1.25 arcseconds, isothermal
Green (lower) = -1.25, thermal gradient, Blue (upper) = +1.25, thermal gradient

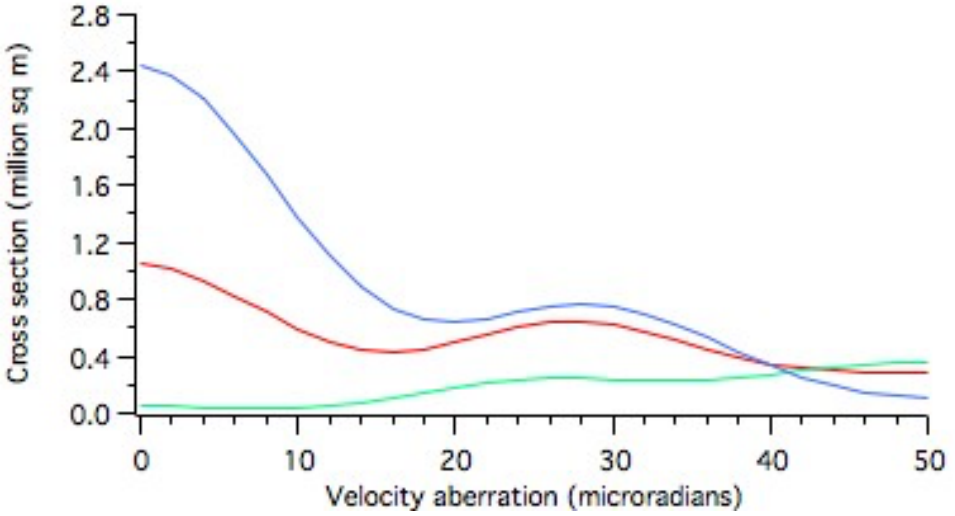

Figure 6.3a.

Microrad	-1.25	+1.25	Diff	Fraction
32	0.23011767	0.70294644	.4728	.6726

Table 6.3a.

Case 16, Program Thermal2
Cube temperature 359 K

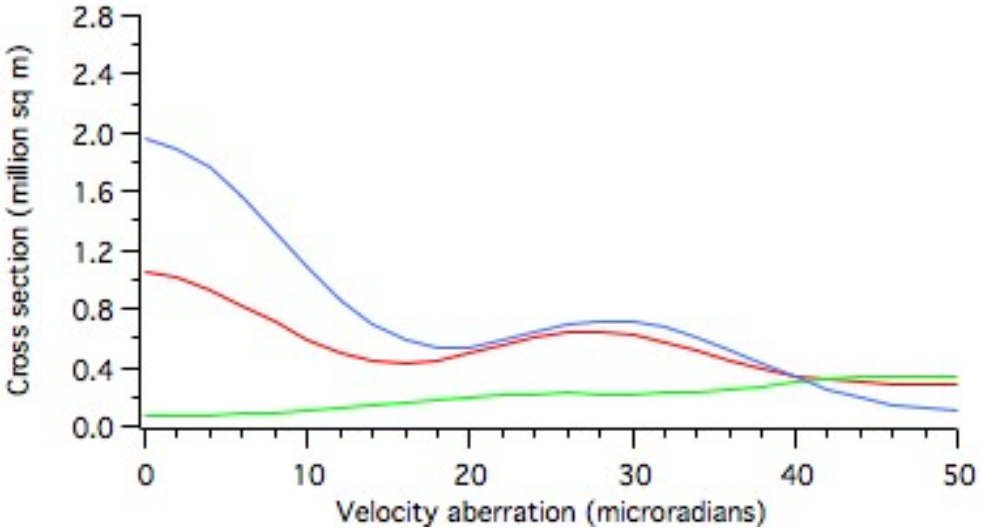

Figure 6.3b.

Microrad	-1.25	+1.25	Diff	Fraction
32	0.22607794	0.67228200	.4462	.6637

Table 6.3b.

Floating mount
Case 17, Italy Program
Cube temperature 298 K, core 343 K, emissivity e=.29
Red (middle) = dihedral angle 1.25 arcseconds, isothermal
Green (lower) = -1.25, thermal gradienst, Blue = +1.25, thermal gradient

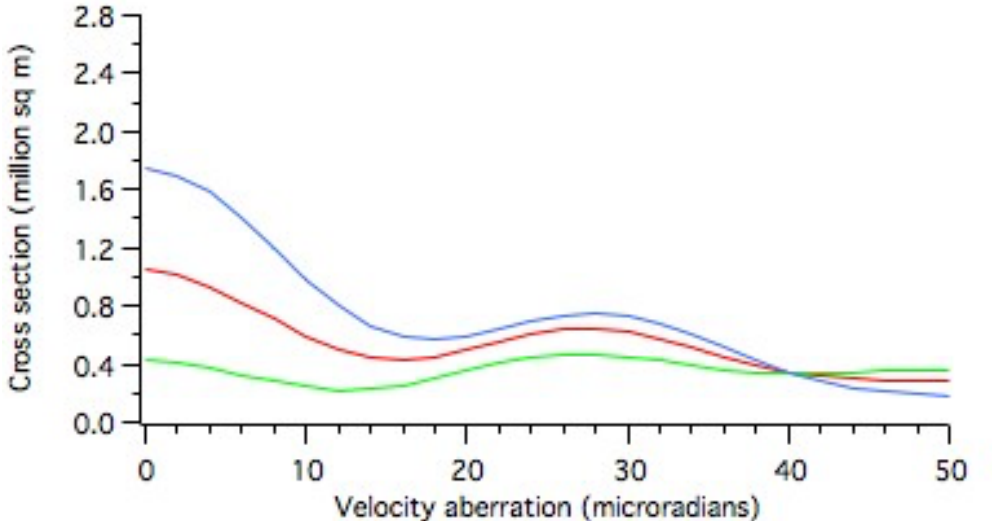

Figure 6.4a.

Microrad	-1.25	+1.25	Diff	Fraction
32	0.42486459	0.67465670	.2498	.3702

Table 6.4a.

Case 17, Program Thermal2
Cube temperature 298 K

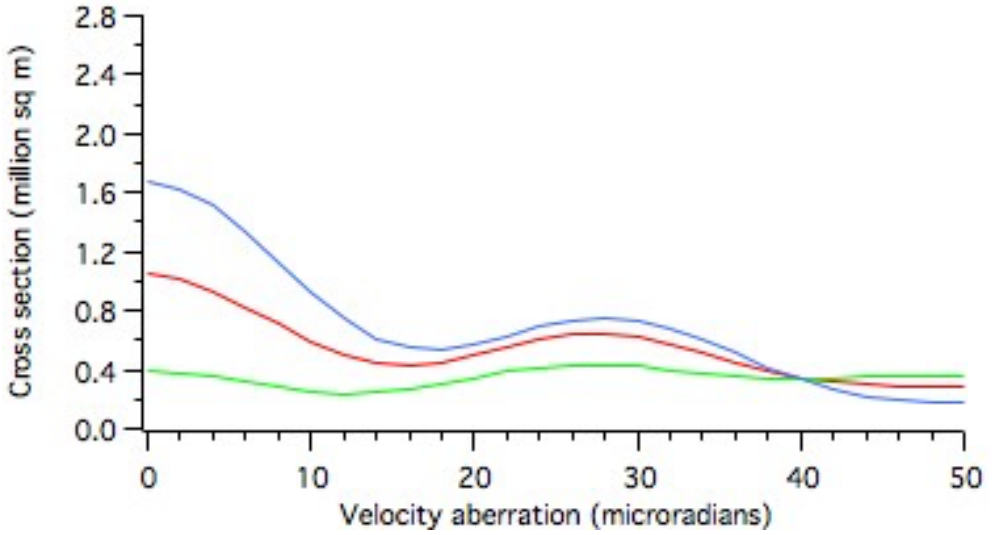

Figure 6.4b.

Microrad	-1.25	+1.25	Diff	Fraction
32	0.39935082	0.68346629	.2841	.4156

Table 6.4b.

Italy program

Fractional change in cross section vs temperature

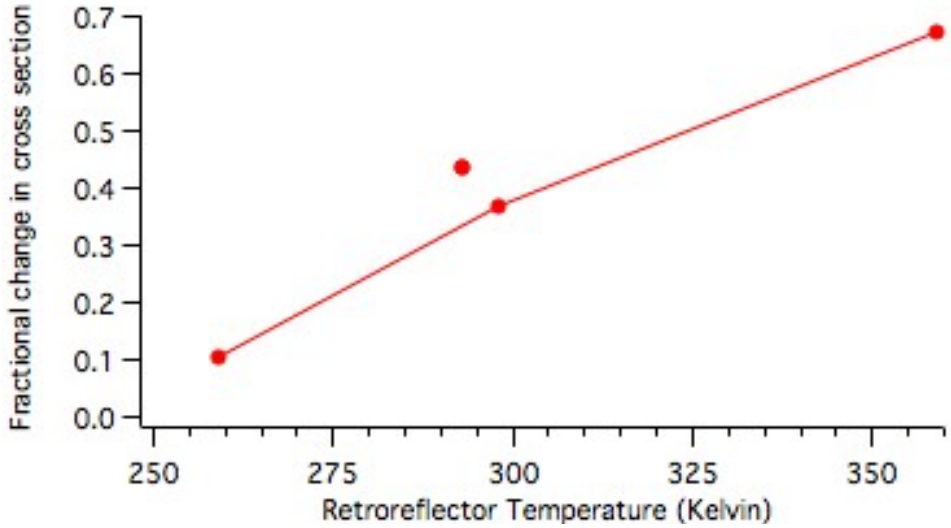

Figure 6.5a.

Case	Core temperature	Reflector Temperature	Fractional change in cross section
11 radiation only	303	259	.1068
17 radiation only	343	298	.3702
16 radiation only	413	359	.6726
12 conduction + radiation	303	293	.4368

Table 6.5.

Temperature vs fractional change in cross section

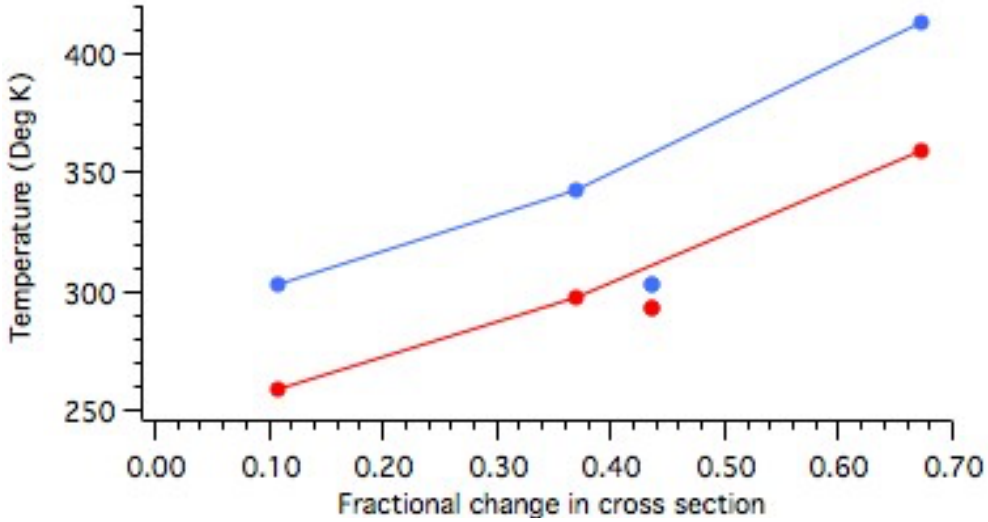

Figure 6.5b.

Red (bottom) = cube temperature, Blue (top) = core temperature, dots = Case 12 with conduction

Program Thermal2

Fractional change in cross section vs temperature

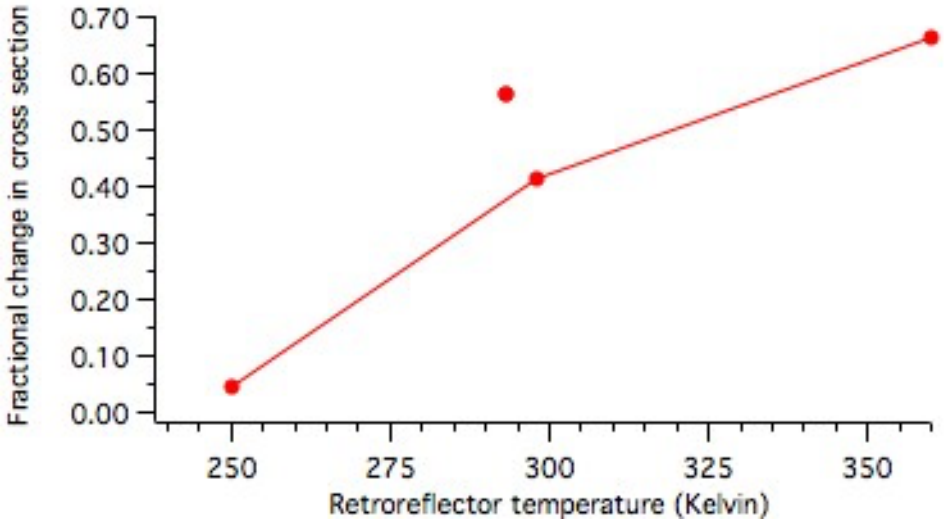

Figure 6.6a

Case	Core temperature	Reflector Temperature	Fractional change in cross section
11 radiation only	303	250	.0444
17 radiation only	343	298	.4156
16 radiation only	413	360	.6637
12 conduction + radiation	303	293	.5653

Table 6.6

Temperature vs fractional change in cross section

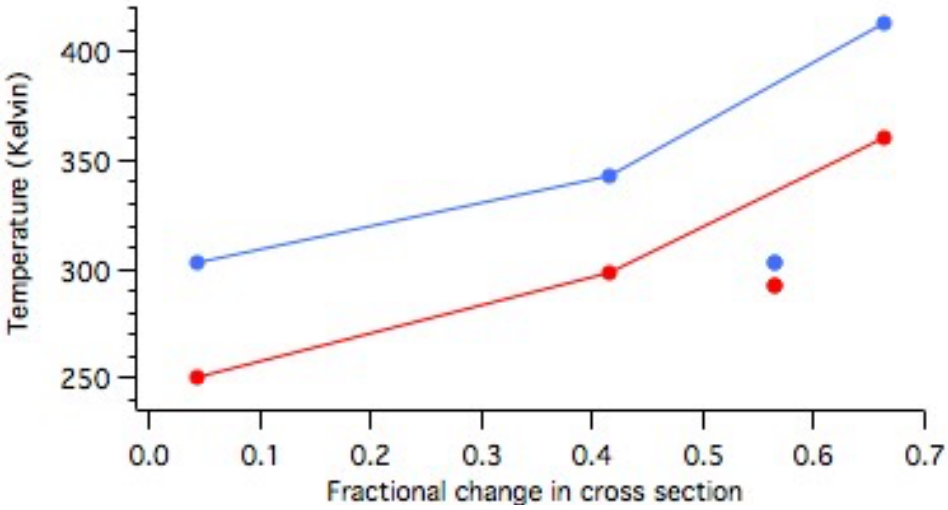

Figure 6.6b

Red = cube temperature, Blue = core temperature, dots = Case 12 with conduction

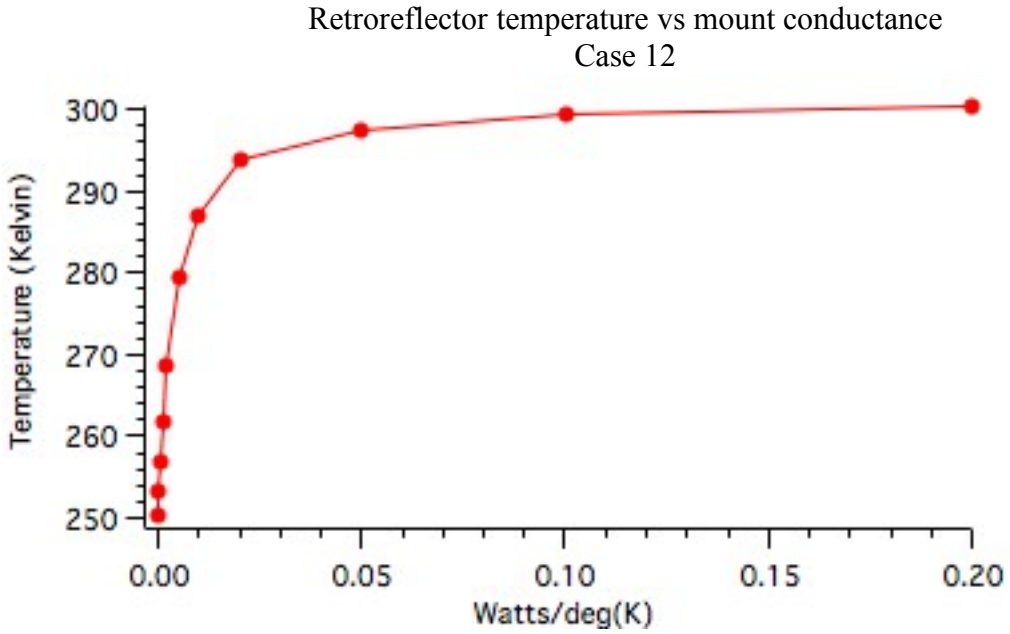

Figure 6.7. Retroreflector temperature vs mount conductance in watts/deg(K)

Mount conductance watts/deg K	Cube temperature K
.0000	250.38
.0002	253.31
.0005	257.00
.0010	261.87
.0020	268.69
.0050	279.40
.0100	286.95
.0200	293.76
.0500	297.48
.1000	299.36
.2000	300.38

Table 6.7

The mount conductance was not specified. However, a value of .020 watts/deg gives the same temperature 293 K as the Italian thermal analysis.

The results show that a very small amount of conductance can have a very significant effect on the temperature of the retroreflector. The effect of the conductance saturates as the temperature of the cube corner approaches the temperature of the cavity and the mounting rings. The floating mount is essential for keeping the cube corner as cold as possible.

The fractional temperature change depends on the cube temperature, not the core temperature. In case 12 the high conductivity brings the cube temperature close to the core temperature. This increases the fractional change in cross section. If the temperature of the cube is below about 250 deg K there should be negligible thermal effects.

Isothermal cross section of a single retroreflector vs dihedral angle offset
Dihedral angle offset = 0.00 to 1.25 arcsec in 0.25 arcsec increments

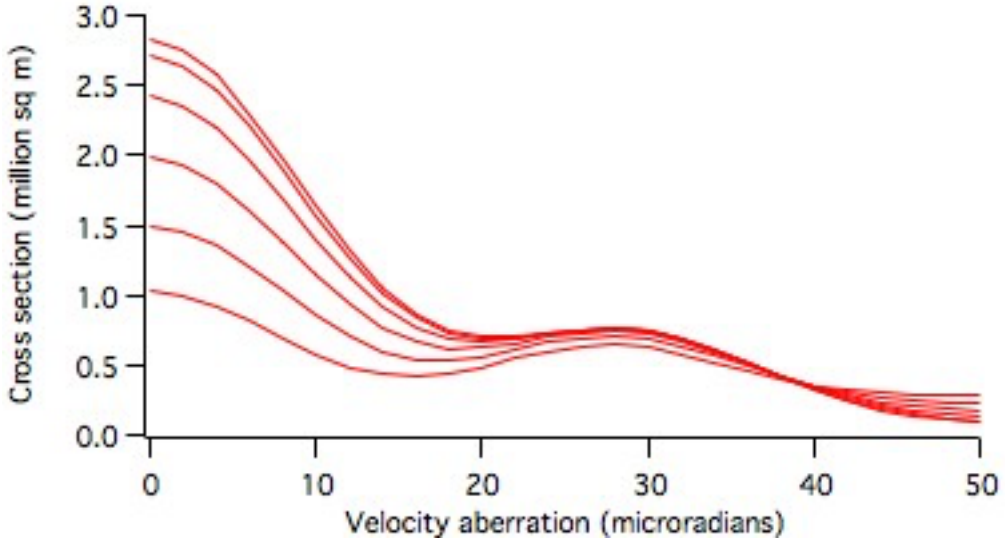

Figure 6.8a.

Expanded plot

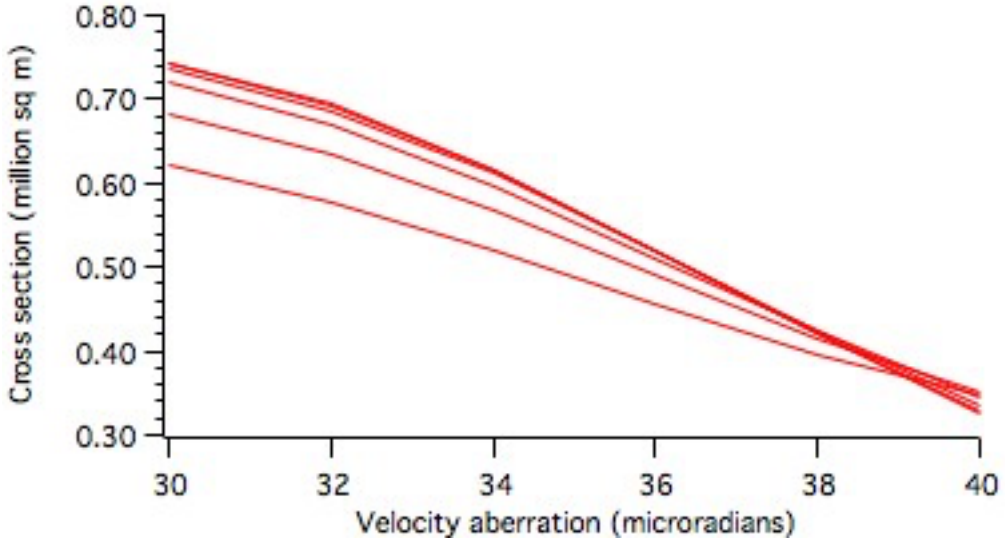

Figure 6.8b. Cross section vs velocity aberration for different dihedral angle offsets

The top curve is with no dihedral angle offset. The bottom curve is with dihedral angle offset = 1.25 arcsec. The change in the cross section with dihedral angle is quite large at the center of the pattern. However, the change at 32 microradians is only about 16 percent. The change at 39 microradians is almost zero.

The change at 32 microradians is still an important difference. If the dihedral angle offset and location on the satellite is recorded for each cube corner it is possible to do an analysis to determine the "as-build" range correction as a function of incidence angle on the satellite.

7. Equations of equilibrium

The thermal simulations show that the cube corner must be kept as cool as possible in order to minimize thermal problems. The temperature of the core and the cube depends on the absorptivity and emissivity of the core, the mounting cavity, and the cube corners. These parameters need to be chosen to minimize the temperature of the cube. If the temperature variations in the core and cube corner are small, it is possible to derive an equation for the temperature of the cubes and the core as follows.

The effective emissivity e_{12} between two infinite parallel plates with emissivity e_1 and e_2 is given by the equation

$$\frac{1}{e_1}+\frac{1}{e_2}-1=\frac{1}{e_{12}} \qquad (1)$$

The thermal radiation from the core to the cube consists of two parts. There is radiation from the retaining rings and radiation directly from the cavity. The total thermal radiation to the cube is

$$R_{core}=\sigma\left(e_{cav}A_{cav}+e_{rings}A_{rings}\right)\left(t_{core}^4-t_{cube}^4\right)$$

where

σ = Stefan Boltzman constant = 5.6697×10^{-8} in MKS units
e_{cav} = the effective emissivity to the core
A_{cav} = the area of the cube that radiates to the core
e_{rings} = the effective emissivity to the rings
A_{rings} = the area of the cube that radiates to the rings
t_{core} = the temperature of the cavity and retaining rings
t_{cube} = the temperature of the cube corner

If we define

$$e_{eff}A_b=e_{cav}A_{cav}+e_{rings}A_{rings}$$

Then we have

$$R_{core}=\sigma e_{eff}A_b\left(t_{core}^4-t_{cube}^4\right) \qquad (2)$$

where

e_{eff} = the effective emissivity between the core and the cube corner
A_b = the total surface area of the back of the cube corner

This initial analysis neglects the mounting rings. Since the radiation from the rings and the cavity differs only by a constant with the same temperature dependence the rings can easily be added to the computation in the term $e_{eff}A_b$.

The temperature of the cube varies by a couple of degrees between the front and the back. Using the average temperature of the cube is adequate for computing the approximate equilibrium temperature.

The heat conducted through the mounting is

$$C_m = c(t_{core} - t_{cube}) \quad (3)$$

where c is the conductance of the mount. The Arthur D. Little report on LAGEOS-1 gives a measured value of 10 milliwats/°K per cube.

The thermal radiation from the front face is

$$R_f = \sigma e_{cube} A_f T_{cube}^4 \quad (4)$$

where
e_{cube} = emissivity of the front face
A_f = the area of the front face

The equilibrium temperature is given by

Heat emitted = heat absorbed

$$\sigma e_{cube} A_f t_{cube}^4 = R_{core} + H_{cube} \quad (5)$$

Where H_{cube} is all other heating such as conduction from the core, solar radiation, and earth infrared.

Substituting Eq. (2) into Eq. (5) gives

$$\sigma e_{cube} A_f T_{cube}^4 = \sigma e_{eff} A_b (t_{core}^4 - t_{cube}^4) + H_{cube} \quad (6)$$

Combining terms we have

$$\left(\sigma e_{eff} A_b + \sigma e_{cube} A_f\right) t_{cube}^4 = \sigma e_{eff} A_b t_{core}^4 + H_{cube} \quad (7)$$

The equilibrium temperature is given by

$$t_{cube}^4 = \frac{\sigma e_{eff} A_b t_{core}^4 + H_{cube}}{\sigma e_{eff} A_b + \sigma e_{cube} A_f} \quad (8)$$

The heat inputs and outputs to the core are:

1. Thermal radiation to the cube.
2. Heat conducted to the cube through the mount.
3. Thermal radiation from the surface not covered by cube corners.
4. Solar radiation.
5. Earth infrared radiation.

Eq. (6) gives the thermal balance for the cube. It gives a relationship between the temperature of the core and the cube. The thermal balance equation for the core is

Heat emitted = heat absorbed

$$\sigma e_{core} A_{core} t_{core}^4 + N R_{core} = H_{core} \quad (9)$$

N is the number of cubes and H_{core} is all other heat transfer such as energy received from solar radiation and earth infrared, and energy transferred to the cube by conduction.

Substituting Eq. (2) into Eq. (9)

$$\sigma e_{core} A_{core} t_{core}^4 + N\sigma e_{eff} A_b (t_{core}^4 - t_{cube}^4) = H_{core} \quad (10)$$

Combining terms,

$$\left(\sigma e_{core} A_{core} + N\sigma e_{eff} A_b\right) t_{core}^4 = N\sigma e_{eff} A_b t_{cube}^4 + H_{core} \quad (11)$$

Eq. (11) is the thermal balance equation for the core. It contains the temperature of the core and the temperature of the cube. Eq. (8) can be used to eliminate the temperature of the cube.

Substituting Eq. (8) into Eq. (11) gives

$$\left(\sigma e_{core} A_{core} + N\sigma e_{eff} A_b\right) t_{core}^4 = N\sigma e_{eff} A_b \frac{\sigma e_{eff} A_b t_{core}^4 + H_{cube}}{\sigma e_{eff} A_b + \sigma e_{cube} A_f} + H_{core} \quad (12)$$

Eq. (12) contains only the temperature of the core. This equation can be solved for the temperature of the core as a functions of the physical constants. Combining terms gives

$$\left[\sigma e_{core} A_{core} + N\sigma e_{eff} A_b \left(1 - \frac{\sigma e_{eff} A_b}{\sigma e_{eff} A_b + \sigma e_{cube} A_f}\right)\right] t_{core}^4 = N\sigma e_{eff} A_b \frac{H_{cube}}{\sigma e_{eff} A_b + \sigma e_{cube} A_f} + H_{core} \quad (13)$$

Cancelling and combining factors of σ gives

$$\sigma\left[e_{core} A_{core} + N e_{eff} A_b \left(1 - \frac{e_{eff} A_b}{e_{eff} A_b + e_{cube} A_f}\right)\right] t_{core}^4 = \frac{N e_{eff} A_b H_{cube}}{e_{eff} A_b + e_{cube} A_f} + H_{core} \quad (14)$$

Simplifying the term in ( ) on the left side we have

$$1 - \frac{e_{eff}A_b}{e_{eff}A_b + e_{cube}A_f} = \frac{e_{eff}A_b + e_{cube}A_f - e_{eff}A_b}{e_{eff}A_b + e_{cube}A_f} = \frac{e_{cube}A_f}{e_{eff}A_b + e_{cube}A_f}$$

Substituting the simplified expression and solving for the core temperature gives

$$t_{core}^4 = \frac{\frac{Ne_{eff}A_bH_{cube}}{e_{eff}A_b + e_{cube}A_f} + H_{core}}{\sigma\left[e_{core}A_{core} + Ne_{eff}A_b\left(\frac{e_{cube}A_f}{e_{eff}A_b + e_{cube}A_f}\right)\right]} \tag{15}$$

The core temperature computed from Eq. (15) can be substituted into Eq. (8) to obtain the cube temperature.

The terms H_{cube} and H_{core} contain the first power of the temperatures according to Eq. (3). If the conduction is zero this equation give the core temperature directly. If the conduction is not zero then an iterative solution is required. With a floating mount there should be negligible conduction between the mount and the cube in space.

8. Temperatures of Core and Cubes

Two cases have been computed. The only heating is solar radiation. The cubes are 1.0 inch diameter. A volumetric solar absorption of 10% is used since the path length in the cube is shorter than in a 1.5 inch cube. The heating is the average over the whole sphere. The solar heating for a cube at normal incidence is divided by 4 to get the average solar heating.

Col	1	2	3	4	5	6	7	8	9	10	11
Case	α_{core}	ε_{core}	ε_{cav}	t_{sphere}	t_{core}	t_{cube}	H_{core}	H_{cube}	R_{core}	R_{ToCube}	R_{cube}
1	.62	.29	.05	338.7	327.6	209.1	75.92	.0177	66.4	.0317	.0494
2	.62	.29	.29	338.7	302.7	252.5	75.92	.0177	49.7	.0874	.1050
3	.15	.80	.05	184.3	183.3	164.6	18.37	.0176	18.4	.0013	.0190
4	.15	.80	.29	184.3	181.0	170.7	18.37	.0177	17.1	.0043	.0220

Table 8.1

Column:
1 Solar absorptivity of the core
2 Emissivity of the core
3 Emissivity of the cavity
4 Temperature of a sphere with no cube corners
5 Temperature of the core
6 Temperature of a cube
7 Solar heating of the core
8 Solar heating of a cube corner
9 Thermal radiation from the core
10 Thermal radiation to a cube corner
11 Radiation from the front face of a cube corner

The amount of heating is independent of the emissivity of the cavity. Changing the emissivity changes the ratio of the heat radiated by the core and the cubes. When the emissivity of the cavity is increased more heat is radiated by the cube corner. The temperature of the core goes down but the temperature of the cube goes up. Column 11 shows the increase in the heat passing through the cube. This is what causes the thermal gradients.

Cases 1 and 2 are for a brushed metal, such as nickel. The thermal constants of nickel from the document "Thermo-Optical Properties" by Isidoro Martinez are absorptivity = .20, and emissivity .05. If nothing is done to the surface of the cavity the emissivity should be .05. If the surface is sand blasted or brushed this can increase the emissivity. It also increases the solar absorptivity. If the emissivity increases more than the absorptivity the net result is to cool the core.

A better approach is shown by Cases 3 and 4. These cases assume some kind of OSR (Optical Solar Reflector, or Second Surface Reflector). Metals tend to have a higher solar absorptivity and lower emissivity as seen in the case of nickel. Metals tend to run hot. Glasses have a low solar absorptivity and a high emissivity. Glasses tend to run cold. In an OSR the solar

radiation passes through a thin layer of glass and is reflected from a metal surface. The metal surface absorbs some of the solar radiation. This heat is conducted to the glass and radiated from the glass. This combination achieves a very low a/e (absorptivity/emissivity) ratio.

In cases 3 and 4 the core and the cubes achieve very low temperatures.

9. Summary.

The use of small cubes eliminates the need for dihedral angle offsets. This allows the use of inexpensive COTS cubes. The small cubes produce a much more accurate isothermal range correction. If the temperature of the cube is less than about 250 deg K the percent change in cross section due to thermal gradients should be negligible. In this case the isothermal range correction will be very close to the actual range correction in orbit.

Specifically, the benefits of using small cubes are:

1. There is more uniform coverage of the surface with smaller variations with incidence angle.

2. The 1.5 inch cubes are too large for the velocity aberration and required dihedral angle offsets. This produces a "lumpy" diffraction pattern that causes variations in range within the far field diffraction pattern.

3. There is an interaction between dihedral angle offsets and the phase changes due to total internal reflection that produces an asymmetrical diffraction pattern when linear polarization is used.

4. The 1.0 inch cubes provide the necessary beam spread to account for velocity aberration without the need for dihedral angle offsets. This also removes the asymmetry in the diffraction pattern with linear polarization.

5. The diffraction pattern without dihedral angle offsets is smoother than the patterns with offsets.

6. The diffraction pattern of an uncoated cube has a ring of spots around the central peak. The size of the cube can be chosen to put the velocity aberration on this ring of spots rather than on a slope in the diffraction pattern. This reduces the variation of the range correction with velocity aberration. This ring of spots is a very stable part of the diffraction pattern that does not change much due to various perturbations.

7. Thermal effects increase as some power (approximately the 4th power) of the size. The reduction in size from 1.5 to 1.0 inches appears to reduce variations in the cross section by about a factor of 5 or 6.

8. Eliminating the dihedral angle offset makes it possible to use COTS (Commercial Off-The-Shelf) cubes that are inexpensive and available quickly. Testing by Ludwig Grunwaldt shows

that the optical quality of these cubes is as good as custom made cubes with dihedral angle offsets that are expensive and time consuming to manufacture.

9. There are small unintentional dihedral angle offsets in COTS cubes that are generally less than one arsec but can be up to two arcsec. The effect of a positive (>90 deg) offset is in the opposite direction from the effect of a negative (<90 deg) offset. Since the mean offset is zero the positive offsets tend to partially cancel the effect of the negative offsets.

10. Thermal simulations show that the effect of thermal gradients in a 1.0 inch cube is very small with a floating mount.

11. A floating mount requires leaving a small gap between the ring and the cube. This could potentially result in damage to the cube due to vibrations during launch. Vibration testing with a very large gap showed no damage to the cube.

12. The thermal simulations show that the fractional change in cross section due to thermal gradients is nearly linear with the temperature of the cube.

10. References.

This paper is self contained. There are no references. The following papers provide additional information related to the contents of this paper.

Arnold, D.A., 1978, Optical and Infrared Transfer Function of the Lageos Retroreflector Array. Technical Report, RTOP 161-05-02, NASA Grant NGR 09-015-002, Supplement No. 57, May. https://ilrs.cddis.eosdis.nasa.gov/docs/1978/Arnold_1978.pdf

Arnold, D.A., 1978, Method of Calculating Retroreflector Array Transfer Functions. Smithsonian Astrophysical Observatory Special Report No. 382, 165 pp. http://www.davidarnoldresearch.org/1979SAO382.pdf

Arnold, D.A., 2015, Transfer Function of the LARES Retroreflector Array. https://ilrs.cddis.eosdis.nasa.gov/docs/2015/Arnold_LaresFinal.pdf

Arnold, D.A., 2017, Transfer Function of the Lageos-2 Retroreflector Array (unpublished). http://www.davidarnoldresearch.org/Lageos-2.pdf